Biochemistry and Biophysics Reports 18 (2019) 100639

Contents lists available at ScienceDirect

Biochemistry and Biophysics Reports

journal homepage: www.elsevier.com/locate/bbrep

Graphene-MoS_2 with TiO_2—SiO_2 layers based surface plasmon resonance biosensor: Numerical development for formalin detection

Md Biplob Hossain[a,*], Md Masud Rana[b], Lway Faisal Abdulrazak[c], Saikat Mitra[b], Mostafizur Rahman[b]

[a] Dept. of Electrical and Electronic Engineering, Jashore University of Science and Technology, Jashore, Bangladesh
[b] Dept. of Electrical & Electronic Engineering, Rajshahi University of Engineering & Technology, Rajshahi, Bangladesh
[c] Dept. of Computer Science, Cihan University-Slemani, Sulaimaniya, Iraq

ARTICLE INFO

Keywords:
ATR
Biosensor
Surface plasmon resonance
Formalin
Resonance angle
Resonance frequency
Graphene
MoS2
TiO2
SiO2

ABSTRACT

In this article, numerically a surface plasmon resonance (SPR) biosensor is developed based on *Graphene-M_OS_2 with TiO_2—SiO_2* hybrid structure for the detection of formalin. Based on attenuated total reflection (ATR) method, we used angular interrogation technique to sense the presence the formalin by observing the change of "minimum reflectance with respect to SPR angle" and "maximum transmittance with respect to surface plasmon resonance frequency (SPRF)". Here, we used Chitosan as probe analyte to perform chemical reaction with formalin (formaldehyde) which is consider as target analyte. Simulation results show a negligible variation of SPRF and SPR angle for improper sensing of formalin that confirms absence of formalin whereas for proper sensing is considerably countable that confirms the presence of formalin. Thereafter, a comparison of sensitivity for different sensor structure is made. It is observed that the sensitivity without TiO_2, SiO_2, MoS_2 and Graphene (conventional structure) is very poor and 73.67% whereas the sensitivity with graphene but without TiO_2, SiO_2 and MoS_2 layers is 74.67% consistently better than the conventional structure. This is due to the electron loss of graphene, which is accompanying with the imaginary dielectric constant. Furthermore, the sensitivity without TiO_2, SiO_2 and graphene but with MoS_2 layer is 79.167%. After more if both graphene and MoS2 are used and TiO_2 and SiO_2 layers are not used then sensitivity improves to 80.5%. This greater than before performance is due to the absorption ability and optical characteristics of graphene biomolecules and high fluorescence quenching ability of MoS_2. Further again, if TiO_2—SiO_2 composite layer is used with the Graphene-MoS2 then the sensitivity enhances from 80.5% to 82.5%. Finally, the sensitivity for the proposed structure has been carried out, and result is 82.83%, the highest value among all the previous structures to integrate the advantages of graphene, MoS_2, TiO_2 and SiO_2.

1. Introduction

Formalin (40% formaldehyde) is a toxic element soluble in water, has been categorized as *Group I* Carcinogen to human beings by the International Agency for Research on Cancer (IRAC) [1]. Recent news has claimed the use of formaldehyde in food preservation that is very popular, particularly in Asian countries [1]. As a result, the finding of formalin is a worried issue which is a biochemical process. Its mechanism of action for fixing lies in its ability to form cross-links between soluble and structural proteins. The resulting structure retains its cellular constituents in them in vivo relationships to each other, giving it a degree of mechanical strength which enables it to withstand subsequent processing, as reported by Environmental and Occupational health and Safely Services 2004 [2].

Today, Biosensors have been penetratingly researched owing to their importance of many industry applications such as medical diagnosis, enzyme detection, food safety and environmental monitoring [3,4]. Today numeral biosensors have been scientifically advanced, among them surface plasmon resonance (SPR) biosensor accepts the advantage of compactness, light weight, high sensitivity, the case of multiplexing and remote sensing and so forth [5]. The SPR sensor works on the basis of attenuated total reflection (ATR) method basically in angular interrogation technique. The ATR method practices a property of total internal reflection (TIR) resulting in a momentary wave normally known as surface plasmon waves (SPW). A beam of incident light is passed through the ATR crystal in such a way that it reflects at least

* Corresponding author. Dept. of Electrical and Electronic Engineering, Jashore University of Science and Technology, Jashore, Bangladesh.
E-mail address: biplobh.eee10@gmail.com (M.B. Hossain).

https://doi.org/10.1016/j.bbrep.2019.100639
Received 31 October 2018; Received in revised form 10 March 2019; Accepted 8 April 2019
Available online 17 April 2019

once off the internal surface in contact with the sample. This reflection forms the momentary wave which extends into the sample [3]. SPW is a momentary guided electromagnetic wave that propagates along a metal-dielectric interface by utilizing the surface plasmon waves (SPW). The variation of the biomolecules concentration on account of chemical reaction, will produce the local modification of the surrounding refractive index (RI) near the sensor surface that outcomes in altering the propagation constant of the SPW and thus the SPR angle and SPR frequency (SPRF) changes [6]. The SPR technique has been successfully applied in various fields, such as chemical and biochemical sensing, film characterization and beam characterization.

Many conventional methods are available for the detection of formalin such as Gas chromatography-mass spectrometry (GC-MS), high performance liquid chromatography (HPLC), fluorimetry, Nash test, gravimetric methods and other chemical based biosensors [7,8,9,10]. Colorimetric detection methods such as Deniges and Eegriwes methods have been known since the beginning of the 20th century [6]. Unluckily, these methods, reagents and reaction products are often just as harmful to human health. All of these conventional methods require similarly hazardous reagents and suffer from a number of interferences, resulting in false positions. Additionally, these methods are impracticable for real time measurements [1].

In this article, numerically *Graphene-M_OS_2 with TiO_2–SiO_2* layer based SPR biosensor is designed for formalin detection by observing the change of SPR angle-minimum reflectance and SPR frequency-maximum transmittance. Here, graphene and MoS_2 are used as biomolecular acknowledgement analytes (BAA), TiO_2–SiO_2 bilayer as the improvement of sensitivity and Gold (Au) as the sharp SPR curve and the oscillation of surface electrons. The enlargement of SPR angle and frequency reasons an increase of SPR performance (sensitivity) [12]. This sensor is identified the presence the formalin based on molecular concentration that is varied due to the immobilization of chitosan (probe analyte) on the sensor surface that changes the RI of sensing analytes. The RI modification will in turn prime to modify in the SPR angle and SPR frequency that explains a final change in propagation constant of SPW [6]. Finally, it is shown that the sensitivity of conventional SPR sensor is 73.67% and the graphene–MoS_2-based sensor is enhanced to 79.167%. with respect conventional SPR sensor. The sensitivity is further enhanced to 82.83%, by including TiO_2–SiO_2 composite layer with respect to conventional SPR sensor. At the end of this letter, a comparative study of the sensitivity of the proposed work with the existing works is discussed.

2. Methodology

A schematic diagram of the proposed composite layered SPR biosensor is shown in Fig. 1. On the basis of kretschmann configuration of SPR, composite layer of Graphene-MoS_2–Au–TiO_2–SiO_2 have deposited on the base of prism and this whole arrangement kept in contact with the PBS or sample containing the target biomolecule/chemical also known as analytes, for sensing application [12]. We used Fresnel seven layered optical system to model the proposed sensor which is elaborately discussed in literature [6,11]. By defining the sensor layers, the first layer is SF11 glass prism (RI, n_p = 1.7786) [12], second layer is TiO_2 (RI, n_2 = 2.5837) [13], third] layer is SiO_2 (RI, n_3 = 1.4570) [12], fourth layer is Au (RI, n_4 = 0.1838 + i*3.4313) [14], fifth layer is MoS_2 (RI, n_5 = 5.9 + i*0.8) [12], sixth layer is graphene (RI, n_6 = 3.0 + i 1.1487) [12] and final layer is Phosphate buffer saline (PBS) solution(RI n_7 = 1.34) as bare sensing dielectric medium that's affords better adsorption of biomolecules [11–21]. After completing the modeling, a TM polarized He–Ne (wavelength = 633 nm) light wave (optical wave) is used to incident as shown in Fig. 1, which passes through the prism and some portion is reflected at the prism-gold interface. During intruding light energy to prism-gold interface, a momentary wave is generated which is known as surface plasmon wave (SPW) mentioning in introduction section. This SPW is reflected at the prism-gold interface. The reflection intensity for TM-polarized light is expressed as [11]:

$$R_p = |r_p|^2 \tag{1}$$

$$\text{Where, } r_p = \frac{(F_{11} + F_{12}n_N)n_1 - (F_{21} + F_{22}n_N)}{(F_{11} + F_{12}n_N)n_1 + (F_{21} + F_{22}n_N)} \tag{2}$$

In equation (2), F is defined as [11].

$$F_{ij} = \left[\prod_{k=2}^{4-1}\begin{pmatrix} \cos\beta_k & -\frac{i\sin\beta_k}{n_k} \\ -in_k\sin\beta_k & \cos\beta_k \end{pmatrix}\right]_{ij} = \begin{bmatrix} F_{11} & F_{12} \\ F_{21} & F_{22} \end{bmatrix} \tag{3}$$

Here n_k is arbitrary transverse refractive indices of the corresponding kth layer which can be explained by the relation [11]:

$$n_k = \left[\frac{\mu_k}{\varepsilon_k}\right]^{1/2}\cos\theta_k = \sqrt{\frac{\varepsilon_k - (n_p\sin\theta_{in})^2}{{\varepsilon_k}^2}} \tag{4}$$

And β_k is arbitrary phase constant of the corresponding kth layer which can be explained by the relation [11]:

$$\beta_k = \frac{2\pi}{\lambda}n_k\cos\theta_k(z_k - z_{k-1}) = \frac{2\pi}{\lambda}d_k\sqrt{\varepsilon_k - (n_p\sin\theta_{in})^2} \tag{5}$$

Here, z_k is the wave impedance of kth layer and is defined as [6]:

$$z_k = \frac{k_{light}n_k\cos\theta_k}{(2\pi c/\lambda_{633}){\varepsilon_k}^2} \tag{6}$$

And θ_k is the incident angle of kth layer, is defined as [6]:

$$\theta_k = a\cos\left(\sqrt{1 - (n_{k-1}/n_k)\sin^2\theta_{in}}\right) \tag{7}$$

In equations (3)–(7), n_p is the RI of prism, θ_{in} is the initial incident angle indicated in equation (1), ε_k is the permittivity of kth layer dielectric, d_k is the thickness of kth layer (thickness of graphene d_g = L × 0.34 nm, where L is the number of graphene layers, thickness of gold d_{Au} = 50 nm) respectively.

The SPW propagates with the dissimilar propagation constant from optical wave which is defined by Eq. (10). The propagation constant of SPW is varied due to the immobilization of formalin (target legend) into chitosan (probe legend which is presence in sensing analytes), and once being equal to the propagation constant of incident light. The point at which incident light propagation constant equals the SPW propagation constant is called SPR point [6]. Eq. (8) depicts that SPR angle is a RI dependent parameter of sensing medium. At SPR point, the frequency at which SPW propagates is called surface plasmon resonance frequency (SPRF) and the angle of incidence is called SPR angle that can be given as follows:

$$\theta_{SPR} = a\sin\sqrt{\frac{n_{com}^2 n_s^2}{n_p^2(n_{com}^2 + n_s^2)}} \tag{8}$$

Here, n_{com} refers equivalent RI of composite layer define as $n_{com} = \sqrt[5]{n_2n_3n_4n_5n_6}$ When formalin is flowing through chitosan on the sensor surface according to Fig. 1, then the RI of sensing medium is modified owing to performing chemical reaction as follows [6]:

$$n_s^2 = n_s^1 + C_a\frac{dn}{dc} \tag{9}$$

Here, n_s^1 is the refractive index (RI) of the sensing dielectric before adsorption of formaldehyde molecules. When no dielectric sample (probe or target) is present inside the sensing medium then n_s^1 is the RI of PBS saline (n_7 = 1.34) which is available in bare sensor. C_a is the concentration of adsorbed bio molecules, for example if 1000 nM concentrated formaldehyde molecules has been added into the sensing medium, then the value of C_a = 1000 nM. The $\frac{dn}{dc}$ is the RI increment parameter, suppose, after adding 1000 nM concentrated formaldehyde molecules, the RI of sensing layer has been changed because the sensing layer now consists not only PBS but also formaldehyde. The changed

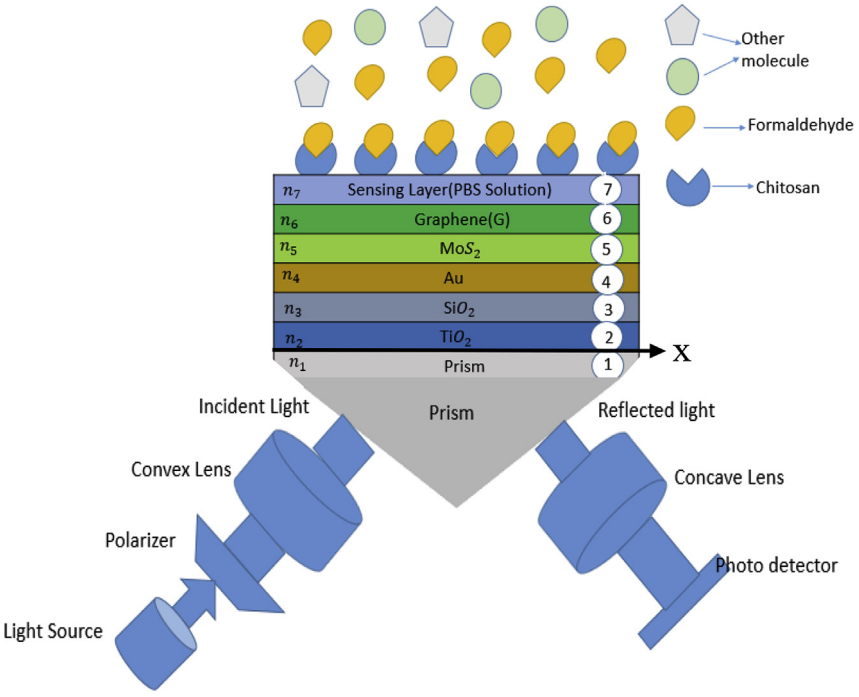

Fig. 1. Schematic of *Graphene-M_OS_2-Au-TiO_2-SiO_2* model for mechanism of formalin detection with hybrid layer biosensor.

value of RI from PBS is $\frac{dn}{dc}$ (= 0.181 cm^3/gm for PBS as bare case [11]). And n_s^2 is the RI of the sensing dielectric after adsorption of formaldehyde molecules.

If SPR angle changes, the propagation constant of SPW also changes which was explained mathematically in the literature [5] as given below:

$$K_{spw} = \frac{2\pi}{\lambda} n_p \sin \theta spr \tag{10}$$

and finally if propagation constant of SPW changes it makes the surface resonance frequency (SPRF) change which can be explained by the following equation:

$$SPRF = \frac{c_o}{n_{com}} \frac{k_{SPW}}{2\pi} \tag{11}$$

Where $\frac{c_o}{n_{com}}$ is the propagation velocity of SPW that is a perpendicularly confined evanescent electromagnetic wave [16,17]. If the incident angle of optical wave is tuned, SPR condition is achieved in which reflectance (R) of reflected wave is minimum and transmittance (T) is maximum and then SPW penetrate at SPF along the x-direction. We define two plot "transmittance versus surface resonance frequency (T ~ SRF curve)," as well as "Reflectance versus surface resonance angle (R ~ SPR-angle curve)," as surface resonance attributor.

3. Numerical results and discussions

Numerical analysis has been initiated to check the routine of proposed sensor by finding it surface plasmon resonance (SPR) angle versus the change of minimum reflectance (R ~ SPR-angle)" attributor and "the surface plasmon resonance frequency (SPRF) versus maximum transmittance (T ~ SPRF)" attributor curve. Fig. 2 (a) and (b), show R ~ SPR-angle and T ~ SPRF curve. The angle of incidence and SPRF of bare sensor are 56.26^0 and 97.968 THz respectively. And the angle of incidence and SPRF while 1000 nM probe chitosan are placed on sensing dielectric, are 56.34^0 and 98.688 THz respectively. Results show no noteworthy change in SPR angle and SPRF (change of SPR angle is 0.08^0, change of SRF is 0.72 THz only) since there no bonding has taken place between probe and target due to the absence of formalin.

Fig. 3 demonstrates the concluding stage of detection concept. It shows, the change of attributor (θsp& R_{min}) and (ΔSPRF & T_{max}) while 1000 nM formaldehyde molecule is sinking in the probe. Results suggest significant change in SPR angle as well as SPRF (58.05^0 and 99.875 THz) due to bonding has taken place between probe (chitosan) and target (formalin). So there is considerable change of charges in target molecule. The change of detecting attributor (θsp & R_{min}) and (ΔSPRF & T_{max}) owing to adding formalin is provided in Table 1. The amount of shift rises with increasing concentration of the detectionable target from 1 to 200 nM as stated by Eq. (9) and tabulated in Table 1. The information of Table 1 has been extracted from Fig. 3(a) and (b).

Table 1 provides information about how θSPR and SPRF parameters change with different concentrations of formalin molecules. It is apparently seen that the considerable increase of SPR angle and SPRF is a sign of bonding between probe and target. Upon making a bond with the target, the chemical configuration of legend is changed, which leads to the change in the optical properties. Hence thus we can observe whether is there formalin in the sample or not. Also increased amount of formalin forms more recurring bonds thus indicating greater interaction [19,20].

For finalizing a decision, at first we measure and tabulate the values of ΔR_{min}^{P-T} and $\Delta\theta_{sp}^{P-T}$ in Table 2 and compare these to threshold values ($(\Delta R_{min}^{P-T})_{\min}$ and $(\Delta\theta_{sp}^{P-T})_{\min}$)If the measured values are greater than these threshold values, then we say there is presence of formalin in the sample. The following equations describe the threshold parameters:

$$(\Delta R_{\min}^{P-T})_{\min} = |R_{\min}^{probe} - R_{\min}^{T\arg et}| = 0.0018 \tag{12}$$

$$(\Delta\theta_{sp}^{P-T})_{\min} = |\theta_{sp}^{P-T} - \theta_{sp}^{T\arg et}| = 1.71 \tag{13}$$

where, $(\Delta R_{min}^{P-T})_{\min}$ is the threshold value of minimum changed reflectance, $(\Delta\theta_{sp}^{P-T})_{\min}$ is the threshold value of changed SPR angle, R_{min}^{Probe}represents the minimum reflectance of probe legend (chitosan), R_{min}^{Target}denotes the minimum reflectance of sampling target, θ_{sp}^{Probe} depicts the SPR angle of probe legend and finally SPR θ_{sp}^{Target} is the SPR angle of sampling target. We reached and tabulated the same calculation by taking $\Delta SPRF_{p-t}$ and ΔT_{max}^{p-t} as also the detecting attributors. The following equations are used to determine the threshold values of these attributors as:

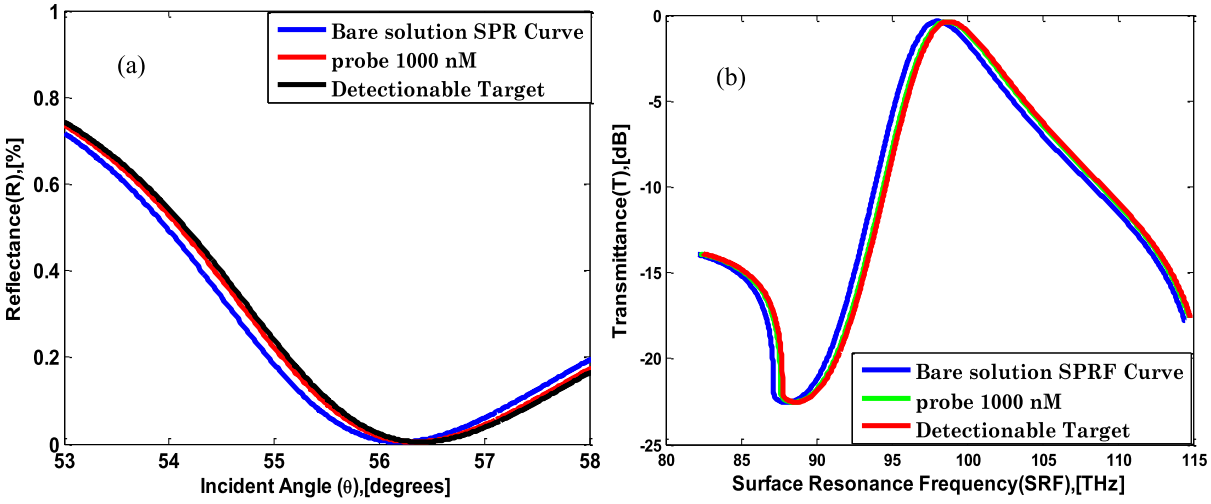

Fig. 2. Numerical results of Bare SPR Sensor (a) R ~ SPR-angle curve in the absence of formalin and chitosan. (b) T ~ SPRF curve in the absence of formalin and chitosan.

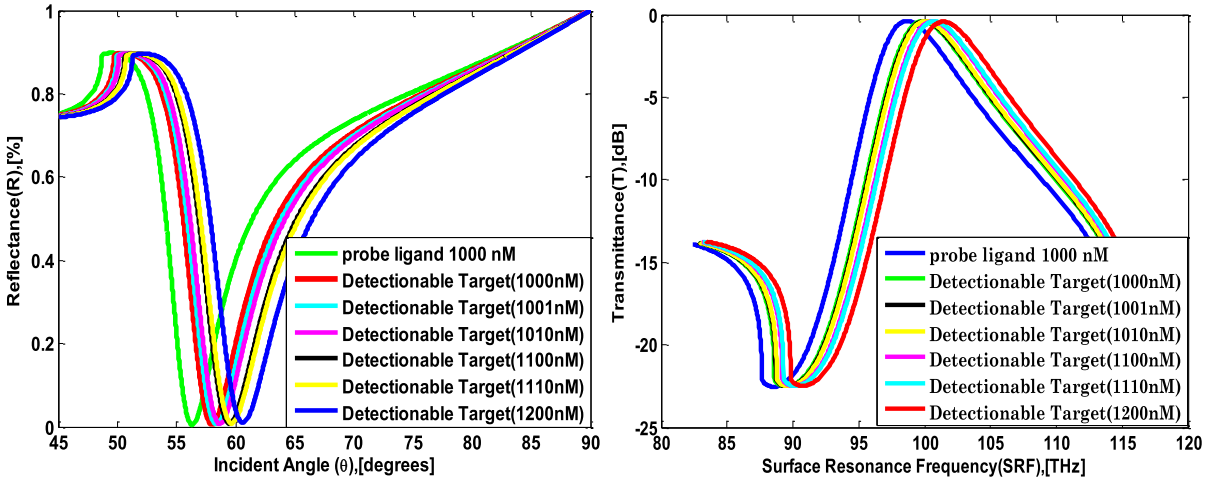

Fig. 3. (a) Reflectance vs. Incident Angle Curve and (b) Transmittance vs. SPR Frequency Curve for Different Concentration of Detectionable Target.

Table 1
R_{min}[%], θ_{SP}[**deg**] , T_{max}[dB] and SPRF[THz] for different concentrated dielectrics medium.

Concentration (C_a) [nM]	R_{min} [%]	θ_{SP}[deg]	T_{max} [dB]	SPRF [THz]
1000 (immobilizer Probe)	0.0044	56.3400	0.3795	98.688
1000 (Detectionable Target)	0.0062	58.0500	0.3981	99.875
1001 (Detectionable Target)	0.0066	58.3800	0.4002	100.008
1010 (Detectionable Target)	0.0070	58.6700	0.4018	100.106
1100 (Detectionable Target)	0.0082	59.4900	0.4106	100.627
1110 (Detectionable Target)	0.0085	59.6800	0.4129	100.761
1200 (Detectionable Target)	0.0100	60.6200	0.4249	101.447

$$(\Delta T_{\max}^{p-t})_{\min} = |T_{\max}^{p} - T_{\max}^{t=1000nm}| = 0.0186 \quad (14)$$

$$(\Delta SRF_{p-t}) = |SRFL_p - SRF_{t=1000nM}| = 1.\ 187 \quad (15)$$

The numerical data judges the strong dependency of the SPR angle and SPRF on the concentration increment that reflects in reflectance and transmittance characteristics curve.

These obtained numerical values can really give an idea about successful interaction or the failed ones. The first condition in Table 3 expresses the desired condition, second and third one needs careful recheck for attaining desired condition, fourth condition confirms the probe is still free from formalin molecule.

Table 2
Calculated ΔR_{min}^{P-T} [%], ΔT_{max}^{p-t} , ΔSRF_{p-t} [THz] and $\Delta\theta_{sp}^{P-T}$ [deg] values from Eq. (5) to Eq. (8) for different concentration of dielectric medium.

Concentration (C_a) [nM]	ΔR_{min}^{P-T}[%] = $\lvert R_{min}^{Probe} - R_{min}^{Target}\rvert$	$\Delta\theta_{sp}^{P-T}$[deg] = $\lvert\theta_{sp}^{Probe} - \theta_{sp}^{Target}\rvert$	ΔT_{max}^{p-t} [dB] = $\lvert T_{max}^{p} - T_{max}^{t}\rvert$	ΔSRF_{p-t} [THz] = $\lvert SRF_p - SRF_t\rvert$
1000 (Target)	$(\Delta R_{min}^{P-T})_{\min}$	$(\Delta\theta_{sp}^{P-T})_{\min}$	$(\Delta T_{\max}^{p-t})_{\min}$	$(\Delta SRF_{p-t})_{\min}$
1001 (Target)	0.0022	2.04	0.0207	1.32
1010 (Target)	0.0026	2.33	0.0223	1.418
1100 (Target)	0.0038	3.15	0.0311	1.939
1110 (Target)	0.0041	3.34	0.0334	2.073
1200 (Target)	0.0056	4.28	0.0354	2.759

Table 3
Four probable conditions for making decision about successful interaction.

Conditions for using & R_{min} as detecting attributor	Conditions for using ΔSPRF & T_{max} as detecting attributor	Decision
$\Delta R_{min}^{P-T} \geq (\Delta R_{min}^{P-T})_{min}$ && $\Delta\theta_{sp}^{P-T} \geq (\Delta\theta_{sp}^{P-T})_{min}$	$\Delta T_{max}^{p-t} \geq (\Delta T_{max}^{p-t})_{min}$ && $\Delta SRF_{p-t} \geq (\Delta SRF_{p-t})_{min}$	Formalin is detected
$\Delta R_{min}^{P-T} \geq (\Delta R_{min}^{P-T})_{min}$ && $\Delta\theta_{sp}^{P-T} \leq (\Delta\theta_{sp}^{P-T})_{min}$	$\Delta T_{max}^{p-t} \geq (\Delta T_{max}^{p-t})_{min}$&& $\Delta SRF_{p-t} \leq (\Delta SRF_{p-t})_{min}$	Re-evaluate
$\Delta R_{min}^{P-T} \leq (\Delta R_{min}^{P-T})_{min}$ && $\Delta\theta_{sp}^{P-T} \geq (\Delta\theta_{sp}^{P-T})_{min}$	$\Delta T_{max}^{p-t} \leq (\Delta T_{max}^{p-t})_{min}$ && $\Delta SRF_{p-t} \geq (\Delta SRF_{p-t})_{min}$	Re-evaluate
$\Delta R_{min}^{P-T} \leq (\Delta R_{min}^{P-T})_{min}$ && $\Delta\theta_{sp}^{P-T} \leq (\Delta\theta_{sp}^{P-T})_{min}$	$\Delta T_{max}^{p-t} \leq (\Delta T_{max}^{p-t})_{min}$&&$\Delta SRF_{p-t} \leq (\Delta SRF_{p-t})_{min}$	Free Probe

Table 4
Arrangement of sensitivity corresponding to sensing layer refractive index from 1.34 to 1.41 for seven different structures at the optimum thickness of TiO2, SiO2 and monolayer of MoS2 and graphene.

Structure configuration	Sensitivity (s) [%RIU^{-1}]							
	n_s^2 = 1.34	n_s^2 = 1.35	n_s^2 = 1.36	n_s^2 = 1.37	n_s^2 = 1.38	n_s^2 = 1.39	n_s^2 = 1.40	n_s^2 = 1.41
Conventional	70.00	70.50	71.33	72.00	72.80	73.67	74.42	75.375
Conventional with Graphene	71.00	71.50	72.33	73.00	73.80	74.67	75.43	76.375
Conventional with MoS2	76.00	75.50	76.33	77.25	78.20	79.167	80.286	81.375
Conventional with Graphene-MoS2	76.50	77.00	77.67	78.50	79.40	80.50	81.43	82.625
Conventional with Graphene-MoS2-TiO2	77.00	78.00	79.00	80.25	81.20	82.50	83.71	85.00
Conventional with Graphene-MoS2-SiO2	76.00	75.90	77.53	78.25	79.00	80.00	81.00	82.00
Conventional with Graphene-MoS2-TiO2-SiO2 (Proposed)	78.00	78.50	79.67	80.50	81.80	82.83	84.00	85.375

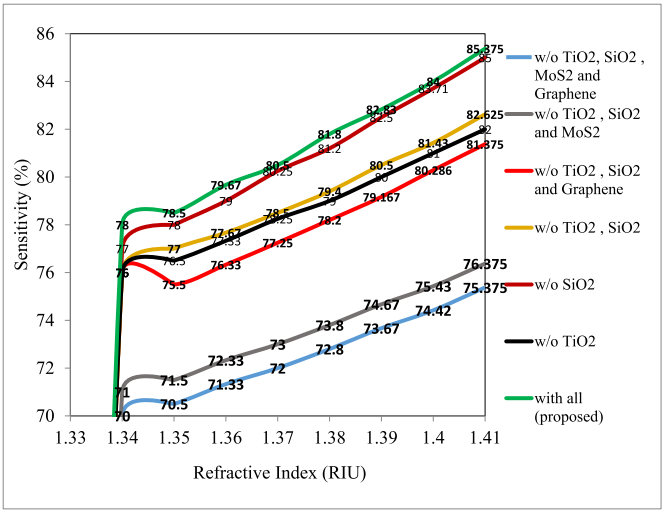

Fig. 4. Sensitivity [%] vs. Refractive Index [RIU] Graph for Different Layer Structure.

The SPR angle increases with the increment of refractive index according to Eq. (1). The variation of sensitivity of the proposed biosensor with respect to the increment of refractive index with a RI step Δn = 0.01 RIU is measured and tabulated in Table 4 and it corresponding results is graphically shown in Fig. 4.

We compare our sensitivity analysis among different sensor structure for 1.39 RIU refractive index which is the changed RI of sensing medium after adsorbing 1000 nM perfectly matched target DNA molecule. From Fig. 4, it can easily be observed that the sensitivity without TiO_2, SiO_2, MoS2 and Graphene (conventional structure) is very poor and 73.67% whereas the sensitivity with graphene but without TiO_2, SiO_2 and MoS_2 layers is 74.67% consistently better than the conventional structure. This is due to the electron loss of graphene, which is accompanying with the imaginary dielectric constant. This increased SPR angle will lead to obtain increased sensitivity of the sensor as sensitivity is directly related to the variation of SPR angle discussed in Ref. [22]. Furthermore, the sensitivity without TiO_2, SiO_2 and graphene but with MoS_2 layer is 79.167%. Because of MoS_2's larger band gap [23], higher optical absorption efficiency [24,25] and larger work function (5.1 eV) as equated with graphene [26]. The sensitivity of the quantum-confinement-incurred direct band gap in MoS_2, allows the high sensitive detection of bio targets. It also holds high fluorescence quenching ability and different affinity in the direction of bio targets [27,28]. After more if both graphene and MoS_2 are used and TiO_2 and SiO_2 layers are not used then sensitivity improves to 80.5%. This greater than before performance is due to the absorption ability and optical characteristics of graphene biomolecules and high fluorescence quenching ability of MoS_2. Further again, if TiO_2—SiO_2 composite layer is used with the Graphene & MoS_2 then the sensitivity enhances from 80.5% to 82.5%. Titanium dioxide (TiO_2) and SiO_2 have purely real refractive index; hence, can be used as adherence layer above the prism base. As an adherence layer, the composite layer performs better than the individual TiO_2 and SiO_2 [29,30] because rich plasmon happens at the TiO_2—SiO_2 interface [31]. And this plasmon enhances light trapping effectively [32] which will generate more surface plasmons (SPs). Due to this more surface plasmons (SPs), which will enhance the SPR angle. This increase in SPR angle will increase the SPR sensitivity. Finally the sensitivity for the proposed structure has been carried out, and result is 82.83%, the highest value among all the previous structures. In order to assimilate the advantages of graphene, MoS_2, TiO_2 and SiO_2, we are motivated to use all of them in a single biosensor, which increases the sensitivity.

Lastly, we feel like making a table showing a comparison of sensitivity of the proposed SPR sensor with other existing. Table 5 has been made with taking into account of sensitivity, on the basis of Structure configuration, and operating wavelength sensors in the literature.

4. Conclusion

In this work, a numerical analysis is reported to observe the effect of adding of graphene, MoS_2, TiO_2 and SiO_2 layer step by step on sensitivity parameters for formalin detection.

The first feature of this study is to detect the presence the formalin based on attenuated total reflection (ATR) method by observing the change of “surface plasmon resonance (SPR) angle versus the change of minimum reflectance” attributor and “the surface plasmon resonance frequency (SPRF) versus maximum transmittance” attributor. Here, Chitosan is used as probe legend to perform particular reaction with the formalin (formaldehyde) as target legend. The second principle feature of this SPR biosensor is the use of graphene, MoS2, TiO2 and SiO2 to

Table 5
Sensitivity of the proposed work and comparison with other existing works.

Structure configuration	Sensitivity [Deg-RIU^{-1}]	Wavelength (nm)	Reference
Conventional with Graphene-MoS2-TiO2-SiO2	82.83	633	In this study
Graphene Coating	57.14	633	[33]
Au-Aluminum thin coating	9.56	680	[34]
Graphene-Ag-Chromium substrate coating	68.03	633	[35]
Au−Ag coating	54.84	632.8	[36]
Graphene Coating	33.98	633	[37]
Graphene Coating with chaclogenide prism	38.88	633	[38]
Transition metal dichalcogenide with silicon nanosheet	89.98	1024	[39]

enhance the sensitivity. The proposed biosensor has a greater sensitivity of 82.83 Deg-RIU^{-1} as compared to the other reported conventional SPR biosensor. Hence, for the first time as per the best of our knowledge, numerical analysis of Graphene-MoS_2-Au−TiO_2-SiO_2 pentasite layer in a single SPR biosensor is proposed.

Conflicts of interest

The authors declare that there is no conflict of interests regarding the publication of this paper.

References

[1] Bohari Noor Aini, KamaruzamanAmpon ShafiquzzamanSiddiquee, Development of formaldehyde biosensor for Determination of formalin in fish samples; malabar red snapper (Lutjanusmalabaricus) and Longtail Tuna (Thunnustonggol)", Biosensors 6 (2016) 32.

[2] Occupational Health and Safety Amendment Regulations, Victorian WorkCover Authority (VWA), 2014 June 2014. Available online: http://www.legislation.vic.gov.au/ accessed on 13 September 2014.

[3] M. Pumera, Graphene in biosensing, Mater. Today 14 (7–8) (2011) 308–315.

[4] J. Homola, Present and future of surface plasmon resonance biosensors, Anal. Bioanal. Chem. 377 (3) (2003) 528–539.

[5] H. Fu, S. Zhang, H. Chen, J. Weng, Graphene enhances the sensitivity of fiber-optic surface plasmon resonance biosensor, IEEE Sens. J. 15 (10) (2015) 5478–5482.

[6] M.B. Hossain, and M.M Rana, "DNA hybridization detection based on resonance frequency readout in graphene on Au spr biosensor", Hindawi Publishing Corporation, J. Sensors, Article no.347595 2016.

[7] N. Noordiana, A.B. Fatimah, Y.C. Farhana, Formaldehyde content and quality characteristics of selected fish and seafood from wet markets, Int. Food Res. J. 18 (2011) 125–136.

[8] I.E. Bechmann, Determination of formaldehyde in frozen fish with formaldehyde dehydrogenase using a flow injection system with an incorporated gel-filtration chromatography column, Anal. Chim. Acta 320 (1996) 155–164.

[9] S. Ngamchana, W. Surareungchai, Sub-millimolar determination of formalin by pulsed amperometric detection, Anal. Chim. Acta 510 (2004) 195–201.

[10] T.S. Yeh, T.C. Lin, C.C. Chen, H.M. Wen, Analysis of free and bound formaldehyde in squid and squid products by gas chromatography-mass spectrometry, J. Food Drug Anal. 21 (2013) 190–197.

[11] M.Saifur Rahman, M.S.Anower, M.Khalilur Rahman,M.RabiulHasan, M. BiplobHossain, M.IsmailHaque, Modeling of a Highly Sensitive MoS2-graphene hybrid based fiber optic SPR biosensor for SensingDNA hybridization, Optik - Int. J. Light Elec. Opt.

[12] J.B. Maurya, Y.K. Prajapati, V. Singh, J.P. Saini, Sensitivity enhancement of surface plasmon resonance sensor based on graphene–MoS2 hybrid structure with TiO2–SiO2 composite layer, Appl. Phys. A 121 (2) (2015) 525–533.

[13] R.C. Jorgenson, S.S. Yee, A fiber-optic chemical sensor based on surface plasmon resonance, Sensor. Actuator. B 12 (1993) 213–220.

[14] J.B. Maurya, Y.K. Prajapati, Rajeev Tripathi, Effect of Molybdenum Disulfide Layer on Surface Plasmon Resonance Biosensor for the Detection of Bacteria" Silicon, (2016).

[15] A. Theisen, C. Johann, M. P. Deacon, S. E. Harding, "Refractive Increment Data-Book for Polymer and Biomolecular Scientist".

[16] R.C. Jorgenson, S.S. Yee, A fiber-optic chemical sensor based on surface plasmon resonance, Sensor. Actuator. B 12 (1993) 213–220.

[17] C. Nylander, B. Liedberg, T. Lind, Gas detection by means of surface plasmons resonance, Sensor. Actuator. 3 (1982) 79–88.

[18] A.J.C. Tubb, F.P. Payne, R.B. Millington, C.R. Lowe, Single mode optical fiber surface plasma wave chemical sensor, Sensor. Actuator. B 41 (1997) 71–79.

[19] U. Fano, J. Opt. Soc. Am. 31 (1941) 213.

[20] R.L. Earp, R.E. Dessy, "Surface Plasmon Resonance", Chapter Contribution in "Commercial Biosensors: Applications to Clinical, Bioprocess, and Environmental Samples", John Wiley and Sons, 1998.

[21] V. Ball, J.J. Ramsden, Buffer dependence of refractive index increments of protein solutions, Biopolymers 46 (7) (Dec. 1998) 489–492.

[22] Design and numerical analysis of highly sensitive Au-MoS2-graphene based hybrid surface plasmon resonance biosensor, (2017).

[23] C.C. Mayorga-Martinez, A. Ambrosi, A.Y.S. Eng, Z. Sofer, M. Pumera, Metallic 1T-WS2 for selective impedimetric vapor sensing, Adv. Funct. Mater. 25 (35) (2015).

[24] A. Ambrosi, Z. Sofer, M. Pumera, 2H/1T phase transition and hydrogen evolution activity of MoS2, MoSe2, WS2 and WSe2 strongly depends on theMX2 composition, Chem. Commun. 51 (40) (2015).

[25] M. O'Brien, K. Lee, R. Morrish, N.C. Berner, N. McEvoy, C.A. Wolden, G.S. Duesberg, Plasma assisted synthesis of WS2 for gas sensing applications, Chem. Phys. Lett. 615 (2014).

[26] Yunhan Luo, Chaoying Chen, Kai Xia, Shuihua Peng, Heyuan Guan, Jieyuan Tang, Huiui Lu, Jianhui Yu, Jun Zhang, Yi Xiao, Zhe Chen, Tungsten disulfide (WS2) based all-fiber-optic humidity sensor, 8956, Optic Express 24 (8) (2016).

[27] H. Shi, H. Pan, Y.W. Zhang, B.I. Yakobson, Quasiparticle band structures and optical properties of strained monolayer MoS2 and WS2, Phys. Rev. B 87 (2013).

[28] J.B. Maurya, Y.K. Prajapati, V. Singh, J.P. Saini, R. Tripathi, Performance of grapheneeMoS2 based surface plasmon resonance sensor using silicon layer, Opt. Quant. Electron. 47 (2015).

[29] S.A. Maier, Plasmonics: Fundamentals and Applications, Springer, 2007.

[30] F. Schedin, Lidorikis Elefterios, Lombardo Antonio, G.K. Vasyl, K.G. Andre, N.G. Alexander, K.S. Novoselov, A.C. Ferrari, Surface-enhanced Raman spectroscopy of graphene, ACS Nano 4 (2010) 5617–5626.

[31] H. Reather, Surface Plasmons on Smooth and Rough Surfaces and on Gratings vol 111, Springer Berlin, 1988.

[32] S.H. Choi, Y.L. Kim, K.M. Byun, Graphene-on-silver substrates for sensitive surface plasmon resonance imaging biosensors, Optic Express 19 (2011) 458–466.

[33] M. Hossain, M. Rana, Graphene coated high sensitive surface plasmon resonance biosensor for sensing DNA hybridization, Sens. Lett. 14 (2) (2016) 145–152.

[34] M. Biednov, T. Lebyedyeva, P. Shpylovyy, Gold and Aluminum based surface Plasmon resonance biosensors: sensitivity enhancement, Proc. Opt. Sensors 9506 (2015) 95061P.

[35] A. Verma, A. Prakash, R. Tripathi, Sensitivity enhancement of surface plasmon resonance biosensor using graphene and air gap, Optic Commun. 357 (2015) 106–112.

[36] L. Xia, S. Yin, H. Gao, Q. Deng, C. Du, Sensitivity enhancement for surface plasmon resonance imaging biosensor by utilizing gold–silver bimetallicfilm configuration, Plasmonics 6 (2011) 245–250.

[37] A. Verma, A. Prakash, R. Tripathi, Performance analysis of graphene based surface plasmon resonance biosensors for detection of pseudomonas-like bacteria, Opt. Quant. Electron. 47 (2015) 1197–1205.

[38] A. Verma, A. Prakash, R. Tripathi, Sensitivity improvement of graphene based surface plasmon resonance biosensors with chaclogenide prism, Optik 127 (2016) 1787–1791.

[39] C.-C. Fong, W.-P. Lai, Y.-C. Leung, S.C.-L. Lo, M.-S. Wong, M. Yang, Study of substrate-enzyme interaction between immobilized pyridoxamine and recombinant porcine pyridoxal kinase using surface plasmon resonance biosensor, Biochim. Et. Biophys. Acta 1596 (1) (2002) 95–107.